Surface modification of Alumina Nanofibres for the Selective Adsorption of Alachlor and Imazaquin Herbicides

Blain Paul, Wayde N. Martens, Ray L. Frost •

Discipline of Chemistry, Queensland University of Technology, Brisbane, Qld 4001, Australia,

Abstract.

The effective removal of pollutants using a thermally and chemically stable substrate that has controllable absorption properties is a goal of water treatment. In this study the surfaces of thin alumina (γ–Al_2O_3) nanofibres were modified by the grafting either of two organosilane agents, 3-chloro-propyl-triethoxysilane (CPTES) and octyl-triethoxysilane (OTES). These modified materials were then trialed as absorbents for the removal of two herbicides, alachlor and imazaquin from water. The formation of organic groups during the functionalisation process established super-hydrophobic sites on the surfaces of the nanofibres. This super hydrophobic group is a kind of protruding adsorption site which facilitates the intimate contact with the pollutants. OTES grafted substrate were shown to be more selective for alachlor while imazaquin selectivity is shown by the CPTES grafted substrate. Kinetics studies revealed that imazaquin was rapidly adsorbed on CPTES modified surfaces. However the adsorption of alachlor by OTES grafted surface was achieved more slowly.

Keywords: Grafted alumina fibres, Adsorption, Water purification, Herbicides, TEM

• Author to whom correspondence should be addressed (r.frost@qut.edu.au)

P:+61 7 3138 2407 F:+61 7 3138 1804

Queensland University of Technology, Faculty of Science and Technology, 2 George St., Brisbane, Queensland Australia 4001

18

19

1. Introduction

There is concern about the existence of commercial herbicides in the environment due to the carcinogenic properties of these compounds. Herbicides are usually released into the environment through the industrial and agricultural operations resulting in them being detected in many surface and ground waters at extremely low concentrations. The removal of these compounds from water may be achieved with a variety of absorbents but the complete removal of these at low concentration is still somewhat difficult [1-9]. This study clearly illustrates that wide range of compounds with varied structures, sizes and functionality can be adsorbed effectively from aqueous systems only by the fine tuning of the adsorption sites [10-16]. It has also been seen that these pollutants exhibit different adsorption properties, with some being strongly adsorbed, whereas others are weakly adsorbed [1, 3]. In general the adsorption behaviour of adsorbents may be affected by many factors. Several investigators have evaluated the importance of the nature of the substrate and its functionalities during adsorption process [12, 13, 17]. Investigations have also been shown that the adsorption of certain solutes increases with an increase in the surface area of the substrate [18, 19].

Porous solids such as activated carbon, natural clays and mesoporous silica possess very high surface area but are poor absorbents due to their the lack of favourable interaction with pollutants. In other words, when predicting the performance of absorbents, it is inadequate to explain the adsorption behaviour only by using the surface area of substrate. The presence of specific functional groups on the surface of the substrate imparts significant characteristics that enhance the adsorption of extremely low concentrations of pollutants. Many researchers have activated substrates by adding functional groups, extensive studies being reported for the adsorption of various pollutants using functionalised clays and mesoporous silica [20-27]. The dependence of the herbicide adsorption capacity of montmorillonite on the existence of pre-adsorbed micelles has been attributed to change in the characteristics of the adsorbents [28]. In some authors suggested the effect of coating on montmorillonite for the adsorption of simazine and its behaviour in solution in the process of adsorption [29]. Mesostructured silica has

also been modified by the incorporation of cyclodextrin for use in the separation of aromatic molecules [30, 31].

When an absorbent is chemically modified is such a way, it is difficult to maintain the stability of the internal pore structures or to get a steady flow rate through the internal channels of the material. The pores of many absorbents are in molecular dimensions so that pollutant molecules penetrating into the channels with bigger size are rejected from pores smaller than this size. When an absorbent is chemically modified, the modifying agent occupies the pore space thereby reducing the total pore volume and the pore diameter. This pore filling reduces the active area for the absorption. On the other hand, the abundance of hydrophobic and protruding adsorption sites enhances the adsorption due to the favourable interaction between the modified sites and the sorbates [32]. In general, the formation of hydrophobic groups on the surface of the substrates during the functionalisation process increases the adsorptive capacity for many pollutants [4, 5, 8, 33, 34]. This increased hydrophobic nature can also reduce the preferential adsorption of water; hence can prevent the blockage of the part of the surface and helps the surface directly interact with the pollutant molecules. It is therefore, reasonable to expect that a stable substrate having certain critical structures and pore diameters can be functionalised with specific organic group leading to extremely high selective sorption capacity toward certain pollutants of low concentration while still maintaining an open porous network allowing high fluid flux.

Various types of oxide nanofibres have been extensively studied by researchers [35-39]. Thin nanofibres of γ–Al_2O_3 poses high surface area, high thermal and chemical stability, and are easily modified on the surface with a large array of long chain organic functional moieties. In this study, the surface modification of γ–Al_2O_3 nanofibres by two different organosilane grafting agents, 3-chloro-propyl-triethoxysilane (CPTES) and octyl-triethoxysilane (OTES), was undertaken and applied to the removal of alachlor and imazaquin from water.

2. Experimental section

2.1. Chemicals

The starting reagents for the preparation of γ–Al_2O_3 nanofibres were polyethylene oxide (PEO) surfactant (Tergitol 15S-7) and $NaAlO_2$ were purchased from Sigma-Aldrich which were both used as received. Acetic acid and hydrochloric acid were obtained from Merck. The organosilane-grafting agents 3-chloropropyltriethoxysilane (CPTES, 99%) and octyltriethoxysilane (OTES, 99%) were purchased from Sigma-Aldrich and were used as served. All other reagents unless otherwise stated, were used as received from Sigma-Aldrich except the toluene (99.8%), which was obtained from Merck and was used after drying (freshly distilled after keeping for 24 h in Na_2CO_3).

2.2. Preparation of γ–Al_2O_3 thin nanofibres and Grafting of functional groups

Thin γ-Al_2O_3 fibres were synthesised by a hydrothermal method and are denoted as AF. These fibres are 5-7 nm thick and 40-60 nm long with a specific surface area of 290 m^2g^{-1}. They were prepared by treating an aluminium hydroxide precipitate with a polyethylene oxide (PEO) surfactant (Tergitol 15S-7 from Aldrich) at 100°C based on the reported work [37, 38]. The reactions were performed in the following manner: 18.8 g of $NaAlO_2$ (0.2 mol of Al) was mixed with 50 mL of 5 M acetic acid solution with continual stirring. The obtained white precipitate was filtered and washed four times in order to remove residual Na ions (pH = 4~5). Aluminium hydrate cake obtained after washing was combined with 40 g PEO surfactant (chemical formula $C_{12\text{-}14}H_{25\text{-}29}O$ $(CH_2CH_2O)_7H$ and an average molecular of weight 508) and stirred to homogenise thoroughly for 4 h. The sticky paste was transferred into a Teflon-lined stainless steel autoclave and heated in an oven at 100 ^oC. The molar ratio of $Al(OH)_3/PEO/H_2O$ was 1:4:16. After two days, fresh aluminium hydrate cake was added to the heating mixture and was stirred for 30 min. The process of adding aluminium hydrate cake continued two more times during a period of two days. The final ratio of $Al(OH)_3/PEO/H_2O$ was 5:1:8, 7.5:1:12 and 10:1:16, respectively for each time. After 8 days of extensive heating in the oven, the reaction mixture led to the

conversion of boehmite fibres. The phase transformation occurred during the calcination of boehmite fibres at 500 ^{o}C to γ-Al_2O_3 nanofibres.

Two different organosilane agents such as 3-chloropropyltriethoxysilane (CPTES) and octyltriethoxysilane (OTES) were chosen to modify the surface after refluxing the γ-Al_2O_3 nanofibres in 0.2 M HCl for 6 h. The acid refluxed fibres are denoted as AF(A). The procedure used for the grafting of γ-Al_2O_3 fibres is described as follows: 1 g of acid treated fibres was placed in a 500 mL flask containing 60 mL dried toluene under stirring, 0.5 mL or 1 mL of CPTES (mass ratio, silane/alumina) was slowly added by means of a syringe. The mixture was refluxed at 120 ^{o}C for 48 h. After cooling, the product was filtered and washed several times with anhydrous enthanol to remove unreacted CPTES and then dried in a vacuum at 110 ^{o}C for 10 h. The resulting material was ground in a mortar and kept in a plastic tube for further characterization and utilization. The modified products were denoted as AFC1(50) (0.5 mL CPTES) and AFC1(100) (1 mL CPTES), respectively. Identical procedures were followed in the case of OTES except that the amount of OTES was 0.57 mL or 1.15 mL. The final materials were denoted as AFC8(50) (0.57 mL of OTES) and AFC8(100) (1.15 mL of OTES), respectively.

2.3. Adsorption test

The experiments were carried out using the batch equilibration method. For each determination, 20 mg of air-dried sample was mixed with 20 ml of alachlor with a concentration range of 2, 4, 6, 8 and 10 ppm respectively in different batches. 1, 2, 3, 4 and 5 ppm concentration ranges were used for imazaquin. Due to the low rate of solubility of herbicides in water the experiments were conducted in lower initial concentrations. The samples were equilibrated for 24 h at room temperature (23 ^{o}C) on a linear shaker in 50 ml polypropylene centrifuge tubes at neutral pH. Following equilibration, the samples were centrifuged, and amounts of pollutants in the supernatant solutions were determined with Varian UV-Vis spectrophotometer Cary 100 with quartz 1 cm cuvettes. The absorbance of alachlor was monitored at 196 nm and imazaquin at 242 nm respectively. Stock standard solution (2, 4, 6, 8, 10

ppm) of alachlor and (1, 2, 3, 4, 5 ppm) were prepared and stored at room temperatures. The amount of herbicide adsorbed was determined by the difference in solution concentrations before and after equilibration. The entire tests performed were completely reproducible.

2.4. Characterisation

XRD patterns were recorded using Cu Kα radiation (n= 1.5418 Å) on a Philips PANalytical X' pert PRO diffractometer operation at 40 kV and 40mA with 0.25^{o} divergence slit, 0.5^{o} antiscatter slit, between 5 and 90^{o} (2θ). The FTIR spectra were acquired using Nicolet FTIR spectrometers Nicolet 380 equipped with Ge/KBr beamsplitter and dGTS/KBr detector. The collection time was about 1 minute (64 scans) for background and sample. The spectrometer was purged with dry air. To prepare KBr pellets, about 2 mg of sample were taken, grinded 1-2 minutes together with about 200 mg of KBr (FT-IR grade, Fluka, dried). The pellets were pressed under vacuum for 4-6 minutes at 8t pressure to produce transparent disks about 1mm thick and 13 mm in diameter. The samples were dried before preparation. An empty KBr pellet was used as reference and its spectrum was subtracted from the sample spectrum to suppress the spectral artifacts caused by KBr impurities and water. Thermal decomposition of the clay samples were carried out in an instrument incorporated with high-resolution thermo gravimetric analyser (series Q500) in a flowing nitrogen atmosphere (60 cm^3/min). Approximately 35 mg of each sample underwent thermal analysis, with a heating rate of 5 ^{o}C/min, with resolution of 6 from 35 ^{o}C to 1000 ^{o}C. Surface analysis based upon the N_2 adsorption/desorption technique was conducted on a micrometrics Tristar 3000 automated gas adsorption analyser after pre-treating the samples at 110 ^{o}C for 12 h under a flow of N_2. Contact Angle was analysed by Nanotech FTA200 Analyser. TEM images were taken using a Philips CM200 TEM with an accelerating voltage of 200 kV. The specimens were deposited onto a copper micro grid coated with a carbon film. Silica magic angle spinning (MAS) NMR spectra were acquired at a magnetic field of 9.4 T with a Varian 400 MHz spectrometer, operating at an excitation frequency of 79.4 MHz for ^{29}Si.

3. Results and discussion

3.1. X-ray diffraction and FTIR Spectra

Figure 1 shows the XRD patterns before and after modification of γ-Al_2O_3 fibres. It can be seen from the XRD patterns that a slight decrease in peak sharpness was observed for the samples after grafting, indicating that there was slight changes in crystallinity after the grafting process. However the overall crystal structure with and without grafting are similar. The standard XRD pattern of γ-Al_2O_3 from JCPDS cards (4-007-2479, 1-74-4629), were used in order to identify the diffraction lines. The calculation of unit cell dimensions indicated that unit cell parameters were not affected after grafting.

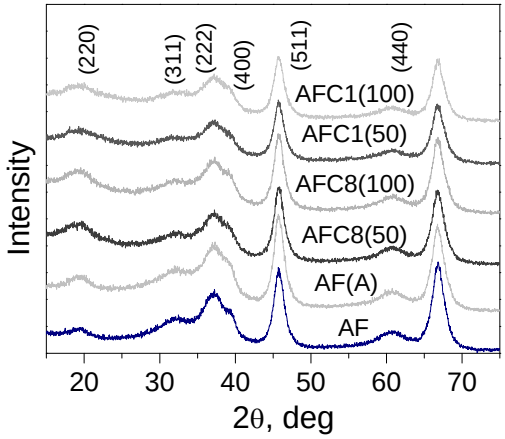

Figure 1. XRD patterns of samples: AF– pure γ-Al_2O_3 fibres; AF(A) – acid washed fibres; AFC8(50) and AFC8(100) – OTES grafted samples; AFC1(50) and AFC1(100) CPTES grafted samples.

Figure 2 displays the FTIR spectra of AF(A), AFC1, and AFC8. Samples AFC1 and AFC8, show bands in the 3000–2700 cm^{-1} region are found to be aliphatic C–H stretching vibrations [40]. Aliphatic CH_2 groups give rise to a doublet at 2938 and 2853 cm^{-1} in the AFC8 spectra, which is assigned to asymmetric and symmetric stretching, respectively.

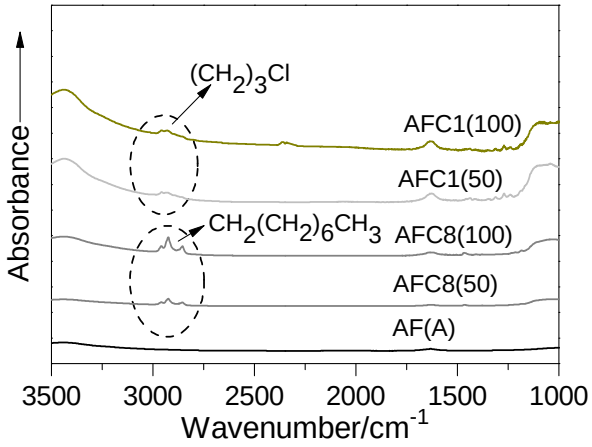

Figure 2. FTIR spectra of samples: AF(A) – acid washed fibres; AFC8(50) and AFC8(100) – OTES grafted samples; AFC1(50) and AFC1(100) CPTES grafted samples.

3.2. TEM image

Figure 3 shows the morphology of nanofibres before and after modification. As seen in the micrograph, functionalisation imparts the aggregation of fibres which can provide fibrillar interstices for the effectiveness of contact time and flow of contaminated water. Formations of these fibrillar interstices are important to improve the efficiency of the sorption.

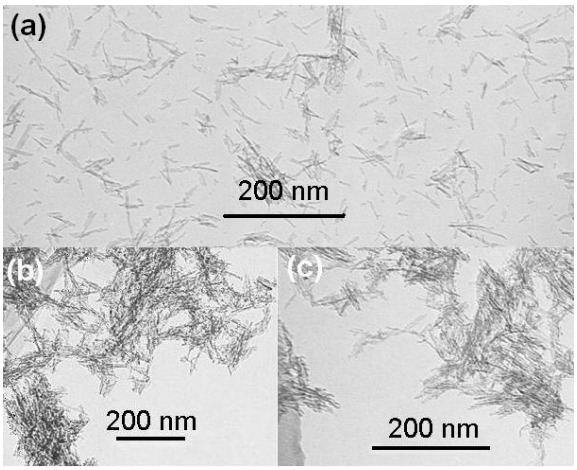

Figure 3. a) Transmission electron micrograph of AF(A); b) and c) micrographs of AFC8(100) and AFCI(100) respectively.

3.3. Thermogravimetric Analysis

Figure 4 shows the mass loss (TG) and the derivative mass loss (DTG) curves of γ-Al_2O_3 samples before and after modification. For the sample AF(A), the mass loss from 36–319 ^oC is assigned to chemically adsorbed water [38]. But in the case of the grafted samples the stages of dehydration are

partially overlapped with the decomposition of the organic species. The major mass loss is in the range of 211–704 °C for AFC8(100) corresponding to the DTG peak at 451 °C. This mass loss is assigned to the degradation of the organic groups. Sample AF(A) illustrated a slightly higher mass loss during the first stage due to the high amount of physically adsorbed water with less hydrophobic surfaces. For the OTES grafted sample AFC8(100), the first stage mass loss is 2% which corresponds to physically adsorbed water. The second stage of mass loss is associated with a very distinct peak and consists of the thermal decomposition of the organic species, which is about 14%. Almost similar mass loss was observed in the sample AFC1(100).

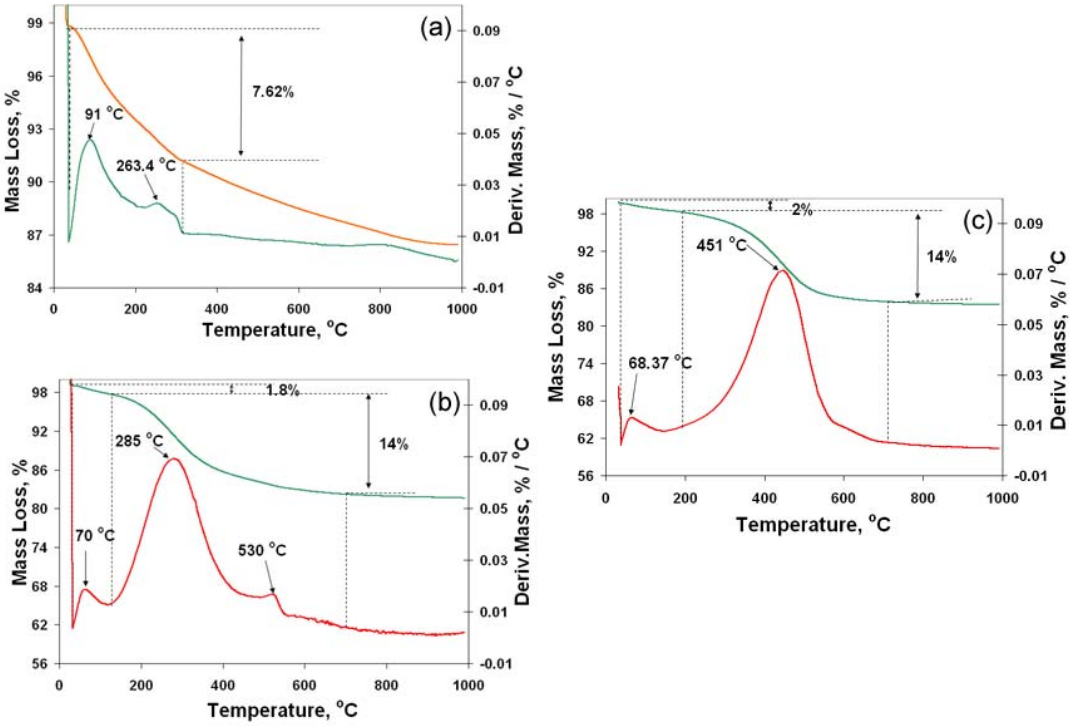

Figure 4. Samples (a) (b) and (c) are TGA and DTG curves of AF(A), AFC1(100) and AFC8(100) respectively.

3.4. Nitrogen adsorption

The nitrogen adsorption isotherms of grafted samples are shown in Figure 5. The isotherms of all the samples exhibit a type IV feature, corresponding to mesoporous materials with capillary condensation. The hysteresis of these samples exhibits the H3 hysteresis loop, which does not exhibit any limiting

adsorption at high P/P_o, and is often observed with aggregates of plate-like particles giving rise to slit-shaped pores [41]. As seen in Figure 5, the isotherm morphology of the grafted samples is similar to that of the non-grafted sample, suggesting the grafting process does not change the feature of the pore structure. However, with the increase of the ratio of organosilane to clay, the specific surface area and porous volume decrease, and the pore diameter slightly increases (Table 1). Apparently, the organic grafting reduces the surface area and the pore volume, which probably resulted from the grafting molecules occupying or blocking the interlayer spacing.

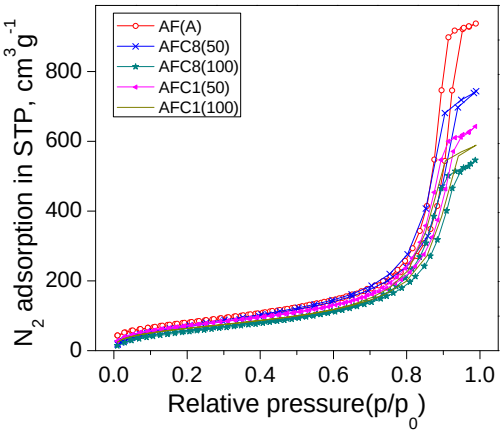

Figure 5. N_2 adsorption/desorption isotherms for grafted and non- grafted γ-Al_2O_3 fibres: AF(A) – acid washed fibres; AFC8(50) and AFC8(100) – OTES grafted samples; AFC1(50) and AFC1(100) – CPTES grafted samples.

Table 1. Specific surface area, pore volume and mean pore diameter of samples: AF and AF (A) as synthesized and acid washed γ-Al_2O_3 respectively; AFC8 (50) and AFC8 (100) – CPTES grafted samples; AFC1 (50) and AFC1 (100) – OTES grafted samples.

			mean D (nm)	
Samples	$S_{BET}(m^2.g^{-1})$	V_p[a]$(cm^3.g^{-1})$	BET[b]	BJH[c]
AF(F)	292	1.450	19.9	14.0
AFC1(50)	266	1.255	14.9	12.5
AFC1(100)	232	1.052	15.7	11
AFC8(50)	252	0.975	16.5	11.4
AFC8(100)	217	0.840	15.3	10.7

[a] Single point adsorption total pore volume of pores at P/P_0 0.99. [b] Adsorption average pore diameter(4V/A by BET). [C] Barrett–Joyner–Halenda(BJH) desorption average pore diameter(4V/A).

3.5. Contact angle

Figure 6 shows the shape of a water droplet on the surface of the tablet form of γ-Al_2O_3 fibre samples. For the acid washed fibres – AF(A), water CA is as low as 18±2º (Figure 6a), displaying a hydrophilic surface. However, as shown in Figure b and c, the water CA of the chloro-propyl group grafted fibres – AFC1(100) increased to 63±2º and the value of octyl group grafted fibres – AFC8(100) is 146±2º. Clearly, the surface modification of fibres leads to a significant change in the polar components therefore resulting in an increase in the contact angle.

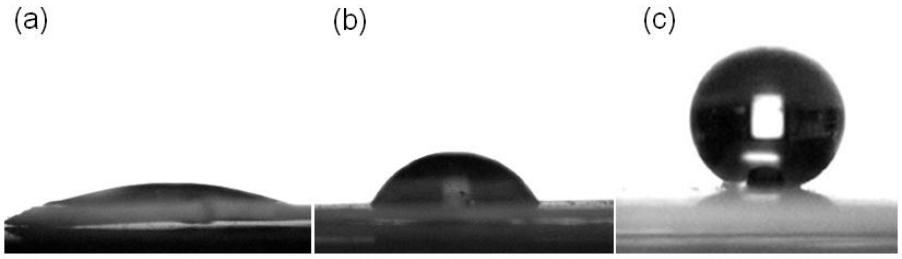

Figure 6. The profile of water droplets on the surface of the pellets form of modified γ-Al_2O_3 fibres: (a) AF(A) – acid washed; (b) AFC1(100) – CPTES grafted samples; (c) AFC8(100) – OTES grafted samples respectively.

3.6. Solid-state ^{29}Si MAS NMR spectra

The following discussion is based on the solid state silicon-29 NMR spectra of modified γ-Al_2O_3 fibres. The formation of a different type of silica environment after grafting was confirmed by the solid-state ^{29}Si MAS NMR spectra (Figures 7). The presence of T_1, T_2 and T_3 signals observed at –76, –67 and –58 corresponding to three different environments of silica atoms in all four samples [42]. T_1, T_2 and T_3 correspond to $[(CH_3CH_2O)_2[43]Si^*(CH_2)_3{-}Cl]$, $[CH_3CH_2O[43]_2Si^*(CH_2)_3{-}Cl]$ and $[AlO)_3Si^*(CH_2)_3{-}Cl]$, respectively for the CPTES grafted γ-Al_2O_3 fibres. Furthermore, the OTES grafted γ-Al_2O_3 fibres, T_1, T_2 and T_3 are correspond to $[(CH_3CH_2O)_2[43]Si^*(CH_2)_7{-}CH_3]$, $[CH_3CH_2O[43]_2Si^*(CH_2)_7{-}CH_3]$ and $[AlO)_3Si^*(CH_2)_7{-}CH_3]$, respectively.

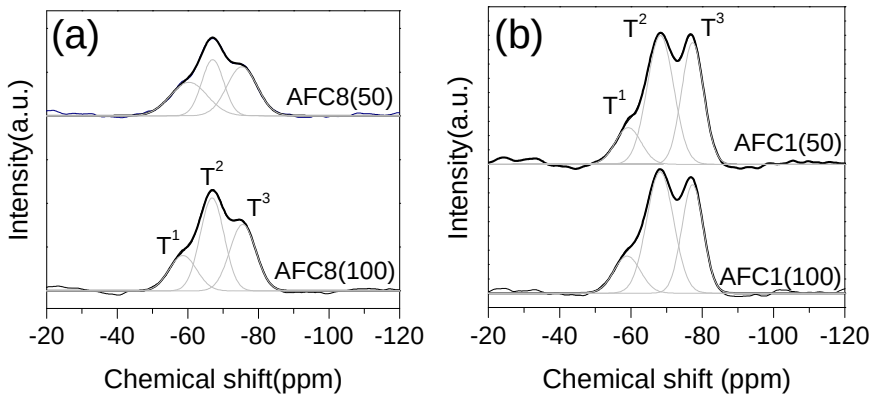

231

232 **Figure 7.** Solid-state ^{29}Si MAS NMR spectra: a) AFC8 – CPTES grafted samples; (b) AFC1 – OTES
233 grafted samples.
234

235 *3.7. Adsorption of herbicides from water*

236 Alachlor and imazaquin are two general use pesticides. The residual alachlor and imazaquin in water
237 could cause environmental problems. The alumina nanofibres grafted with functional groups were used
238 as sorbents to remove trace alachlor and imazaquin from water and is schematically represented in the
239 Figure 8.

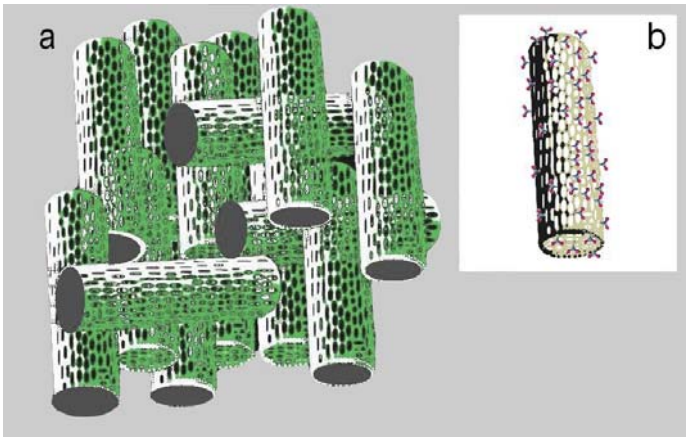

240

241 **Figure 8.** The schematical diagrams of γ-Al_2O_3 fibres before (a) and after grafting (b).
242

243 The contact angle measurements show that the majority of the fibres surface was converted to a
244 hydrophobic surface after the grafting process (Figure 6). As a result, the hydrophobic region of the
245 surface can make close proximity with the hydrophobic part of the adsorbed molecule. The main
246 advantage of using fibre as absorbent was their easy separation from solutions after the adsorption

process. Sorption isotherms of differently modified fibres were shown in Figure 9. The grafted nanofibres exhibit a very high adsorption ability when compared to non-grafted γ-Al_2O_3 fibres. Sample AFC8(100) can absorb 1.6 mg/g alachlor at an initial lower amount of 2 mg/g and sample AFC1(100) can absorb imazaquin about 1 mg/g of adsorbent at an initial lower amount of 1 mg/g. It was also recognized that the rate of adsorption of imazaquin by CPTES was very high.

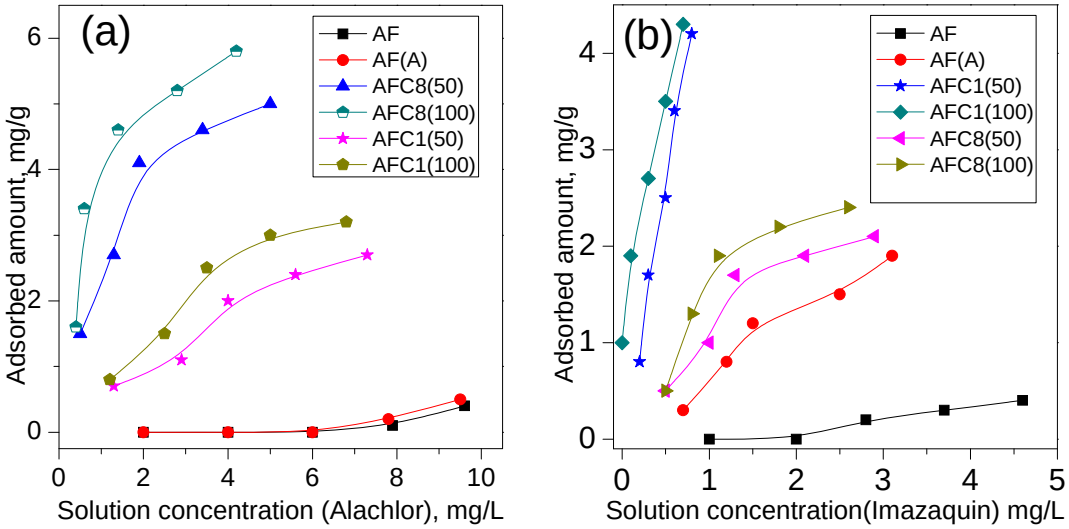

Figure 9. Adsorption isotherms of alachlor(a) and Imazaquin(b)

The linear part of the isotherms reflects the situation at low concentrations where the adsorption sites are far from being filled. The curves of the isotherms show that it becomes more difficult to adsorb additional molecules. As seen in Figure 9, the adsorption isotherm of alachlor for AFC8 (100) is also type H and the linearity of type C adsorption isotherm of imazaquin for AFC1(100) and AFC1(50) shows that the availability of more sites depend on how the adsorption proceeds [44]. The kinetics of uptake of the two pesticides was measured to evaluate the time needed to reach adsorption equilibrium. The rate of adsorption was measured by determining the change in concentration of the pollutants in contact with the adsorbent as a function of time. The sorbed amounts of pollutants were then plotted against the square root of time (Figure 10).

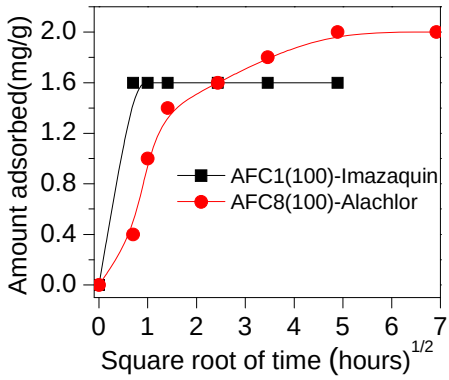

Figure 10. The amount of uptake were plotted against the square root of time.

Imazaquin was adsorbed readily by AFC1(100), reaching the adsorption equilibrium within 30 min whereas, a slow rate of adsorption was measured for alachlor by AFC8(100) with complete equilibrium being achieved only after 24 h. The adsorption mechanism is assumed to be proceeded in a multi-steps process. In the first step, the pollutant molecules transport from solution to the hydrophobic surfaces of alumina fibres. Secondly, the solute molecules diffuse into hydrophobic nanospaces and finally the adsorption process takes place. The small size of alachlor compared with imazaquin, allows its easy adsorption on to the OTES grafted substrate which is mainly due to the hydrophobic interactions of the methyl groups present in the grafted species as well as in the alachlor molecules. Furthermore, molecules with larger number of hydrophobic alkyl groups are preferentially adsorbed. It is believed that the enhanced adsorption rate of imazaquin was determined by the hydrophobicity of alkyl groups as well as due to the large number of π bonding electrons in the imazaquin molecules. Hydrogen bonding plays a prominent role in the mechanism of the last step adsorption process (Figure 11). It involves the interactions of aromatic π electron ring and the chlorine groups in a donor-acceptor mechanism take place through chlorine as an electron donor and an aromatic ring as the acceptor [45].

280 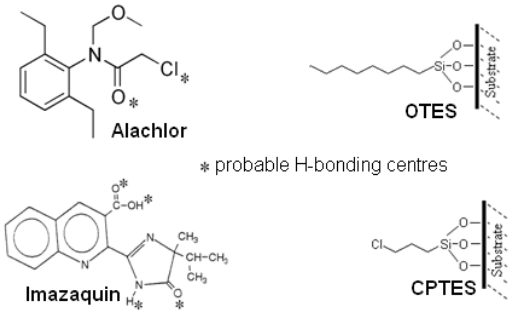

281 **Figure 11.** A schematical view of grafted surface and possible interaction with pollutants.

282 Intermolecular hydrogen bonds exist between the fibres providing cohesion of the fibrillar units. Indeed,
283 these cohesive forces in the fibrillar interstices have a pronounced effect on the accessibility and the
284 interactions of pollutants with the fibre. The aggregation of fibrils attributes the easy and high speed of
285 the downstream separation.

286 **4. Conclusions**

287 Adsorption characteristics of functionalised thin γ-Al_2O_3 fibres were examined in batch processes.
288 The efficiency of alachlor and imazaquin removal from water after grafting γ-Al_2O_3 fibres are
289 significantly higher than that of non-grafted fibres. It was seen that these modified fibres exhibit
290 different adsorption characteristics, i.e., some are strongly adsorbed whereas others are weakly adsorbed
291 depends on the functionalities. γ-Al_2O_3 fibres modified with OTES can absorb alachlor 1.6 mg/g of
292 adsorbent at an initial lower concentration of 2 mg/g and CPTES grafted γ-Al_2O_3 fibres can absorb
293 imazaquin about 1 mg/g of adsorbent at an initial concentration of 1 mg/g. A higher selectivity of
294 imazaquin was observed for CPTES in comparison with OTES and an opposite effect was associated
295 with alachlor uptake. After evaluating the kinetics of uptake, it was observed that CPTES grafted fibres
296 could remove imazaquin much quicker than alachlor by OTES modified substrate. The surface
297 modification provided a relatively large number of highly hydrophobic sites and a super-hydrophobicity
298 was observed in the OTES system. Organically modified products were analyzed by FTIR disclosed the
299 existence of organic groups and also there is a significant decrease in the surface area after grafting by

300 BET. XRD measurements indicated that grafting has no influence in the crystal structure of the
301 substrate.

302 **Acknowledgments**

303 This work was supported by Australian Research Council (ARC). The author is grateful to Prof. H.Y.
304 Zhu and Dr. Dongjiang Yang for their aid in the data analysis.

305

306 **References**

307 [1] S. Nir, T. Undabeytia, D. Yaron-Marcovich, Y. El-Nahhal, T. Polubesova, C. Serban, G. Rytwo, G.
308 Lagaly, B. Rubin, Optimization of Adsorption of Hydrophobic Herbicides on Montmorillonite
309 Preadsorbed by Monovalent Organic Cations: Interaction between Phenyl Rings, Environmental
310 Science & Technology, 34 (2000) 1269-1274.
311 [2] T. Polubesova, Y. Chen, R. Navon, B. Chefetz, Interactions of hydrophobic fractions of dissolved
312 organic matter with Fe^{3+} and Cu^{2+} montmorillonite, Environmental Science & Technology, 42 (2008)
313 4797-4803.
314 [3] T. Polubesova, S. Nir, D. Zadaka, O. Rabinovitz, C. Serban, L. Groisman, B. Rubin, Water
315 Purification from Organic Pollutants by Optimized Micelle-Clay Systems, Environmental Science &
316 Technology, 39 (2005) 2343-2348.
317 [4] J.A. Smith, A. Galan, Sorption of Nonionic Organic Contaminants to Single and Dual Organic
318 Cation Bentonites from Water, Environmental Science & Technology, 29 (1995) 685-692.
319 [5] J.A. Smith, P.R. Jaffe, C.T. Chiou, Effect of ten quaternary ammonium cations on
320 tetrachloromethane sorption to clay from water, Environmental Science & Technology, 24 (1990) 1167-
321 1172.
322 [6] J. Wei, G. Furrer, S. Kaufmann, R. Schulin, Influence of Clay Minerals on the Hydrolysis of
323 Carbamate Pesticides, Environmental Science & Technology, 35 (2001) 2226-2232.
324 [7] L. Zhu, B. Chen, X. Shen, Sorption of Phenol, p-Nitrophenol, and Aniline to Dual-Cation
325 Organobentonites from Water, Environmental Science & Technology, 34 (2000) 468-475.
326 [8] J.A. Smith, P.R. Jaffe, Benzene Transport through Landfill Liners Containing Organophilic
327 Bentonite, Journal of Environmental Engineering-Asce, 120 (1994) 1559-1577.
328 [9] T. Polubesova, S. Nir, Z. Gerstl, M. Borisover, B. Rubin, Imazaquin adsorbed on pillared clay and
329 crystal violet-montmorillonite complexes for reduced leaching in soil, Journal of Environmental
330 Quality, 31 (2002) 1657-1664.
331 [10] F. De Juan, E. Ruiz-Hitzky, Selective functionalization of mesoporous silica, Advanced Materials,
332 12 (2000) 430-432.
333 [11] J.C. Dai, J.T. Huang, Surface modification of clays and clay-rubber composite, Applied Clay
334 Science, 15 (1999) 51-65.
335 [12] L. Groisman, C. Rav-Acha, Z. Gerstl, U. Mingelgrin, Sorption of organic compounds of varying
336 hydrophobicities from water and industrial wastewater by long- and short-chain organoclays, Applied
337 Clay Science, 24 (2004) 159-166.
338 [13] D. Zadaka, Y.G. Mishael, T. Polubesova, C. Serban, S. Nir, Modified silicates and porous glass as
339 adsorbents for removal of organic pollutants from water and comparison with activated carbons,
340 Applied Clay Science, 36 (2007) 174-181.
341 [14] K.A. Carrado, L.Q. Xu, R. Csencsits, J.V. Muntean, Use of organo- and alkoxysilanes in the
342 synthesis of grafted and pristine clays, Chemistry of Materials, 13 (2001) 3766-3773.
343 [15] J.J. Tunney, C. Detellier, Interlamellar Covalent Grafting of Organic Units on Kaolinite, Chemistry
344 of Materials, 5 (1993) 747-748.
345 [16] P.A. Wheeler, J.Z. Wang, J. Baker, L.J. Mathias, Synthesis and characterization of covalently
346 functionalized laponite clay, Chemistry of Materials, 17 (2005) 3012-3018.
347 [17] N. Masque, R.M. Marce, F. Borrull, Comparison of different sorbents for on-line solid-phase
348 extraction of pesticides and phenolic compounds from natural water followed by liquid
349 chromatography, Journal of Chromatography A, 793 (1998) 257-263.
350 [18] D. Clifford, S. Subramonian, T.J. Sorg, Water treatment processes. III. Removing dissolved
351 inorganic contaminants from water, Environmental Science & Technology, 20 (2002) 1072-1080.
352 [19] S.B. Haderlein, K.W. Weissmahr, R.P. Schwarzenbach, Specific Adsorption of Nitroaromatic
353 Explosives and Pesticides to Clay Minerals, Environmental Science & Technology, 30 (1996) 612-622.
354 [20] R. Celis, M.C. Hermosin, J. Cornejo, Heavy metal adsorption by functionalized clays,
355 Environmental Science & Technology, 34 (2000) 4593-4599.

[21] L. Cox, R. Celis, M.C. Hermosin, J. Cornejo, A. Zsolnay, K. Zeller, Effect of organic amendments on herbicide sorption as related to the nature of the dissolved organic matter, Environmental Science & Technology, 34 (2000) 4600-4605.
[22] X. Feng, G.E. Fryxell, L.Q. Wang, A.Y. Kim, J. Liu, K.M. Kemner, Functionalized monolayers on ordered mesoporous supports, Science, 276 (1997) 923-926.
[23] J. Liu, X.D. Feng, G.E. Fryxell, L.Q. Wang, A.Y. Kim, M.L. Gong, Hybrid mesoporous materials with functionalized monolayers, Advanced Materials, 10 (1998) 161-165.
[24] L. Mercier, T.J. Pinnavaia, Access in mesoporous materials: Advantages of a uniform pore structure in the design of a heavy metal ion adsorbent for environmental remediation, Advanced Materials, 9 (1997) 500-503.
[25] H. Yoshitake, T. Yokoi, T. Tatsumi, Adsorption behavior of arsenate at transition metal cations captured by amino-functionalized mesoporous silicas, Chemistry of Materials, 15 (2003) 1713-1721.
[26] J. Brown, L. Mercier, T.J. Pinnavaia, Selective adsorption of Hg^{2+} by thiol-functionalized nanoporous silica, Chemical Communications, (1999) 69-70.
[27] A.M. Liu, K. Hidajat, S. Kawi, D.Y. Zhao, A new class of hybrid mesoporous materials with functionalized organic monolayers for selective adsorption of heavy metal ions, Chemical Communications, (2000) 1145-1146.
[28] T. Polubesova, S. Nir, D. Zadaka, O. Rabinovitz, C. Serban, L. Groisman, B. Rubin, Water purification from organic pollutants by optimized micelle-clay systems, Environmental Science & Technology, 39 (2005) 2343-2348.
[29] F. Sannino, M.T. Filazzola, A. Violante, L. Gianfreda, Adsorption-desorption of simazine on montmorillonite coated by hydroxy aluminum species, Environmental Science & Technology, 33 (1999) 4221-4225.
[30] R. Huq, L. Mercier, P.J. Kooyman, Incorporation of cyclodextrin into mesostructured silica, Chemistry of Materials, 13 (2001) 4512-4519.
[31] A. Bibby, L. Mercier, Adsorption and separation of water-soluble aromatic molecules by cyclodextrin-functionalized mesoporous silica, Green Chemistry, 5 (2003) 15-19.
[32] D.J. Yang, B. Paul, W.J. Xu, Y. Yuan, E.M. Liu, X.B. Ke, R.M. Wellard, C. Guo, Y. Xu, Y.H. Sun, H.Y. Zhu, Alumina nanofibers grafted with functional groups: A new design in efficient sorbents for removal of toxic contaminants from water, Water Research, 44 741-750.
[33] S.A. Boyd, M.M. Mortland, C.T. Chiou, Sorption Characteristics of Organic Compounds on hexadecyltrimethylammonium-Smectite, Soil Science Society of America Journal 52 (1988) 652-657.
[34] J.A. Smith, P.R. Jaffe, Adsorptive Selectivity of Organic-Cation-Modified Bentonite for Nonionic Organic Contaminants, Water Air and Soil Pollution, 72 (1994) 205-211.
[35] Zhu, Gao, Y. Lan, Song, Xi, Zhao, Hydrogen Titanate Nanofibers Covered with Anatase Nanocrystals: A Delicate Structure Achieved by the Wet Chemistry Reaction of the Titanate Nanofibers, Journal of the American Chemical Society, 126 (2004) 8380-8381.
[36] S.C. Shen, Q. Chen, P.S. Chow, G.H. Tan, X.T. Zeng, Z. Wang, R.B.H. Tan, Steam-Assisted Solid Wet-Gel Synthesis of High-Quality Nanorods of Boehmite and Alumina, The Journal of Physical Chemistry C, 111 (2006) 700-707.
[37] H.Y. Zhu, X.P. Gao, D.Y. Song, Y.Q. Bai, S.P. Ringer, Z. Gao, Y.X. Xi, W. Martens, J.D. Riches, R.L. Frost, Growth of Boehmite Nanofibers by Assembling Nanoparticles with Surfactant Micelles, The Journal of Physical Chemistry B, 108 (2004) 4245-4247.
[38] H.Y. Zhu, J.D. Riches, J.C. Barry, Alumina Nanofibers Prepared from Aluminum Hydrate with Poly(ethylene oxide) Surfactant, Chemistry of Materials, 14 (2002) 2086-2093.
[39] Y. Xia, P. Yang, Guest Editorial: Chemistry and Physics of Nanowires, Advanced Materials, 15 (2003) 351-352.
[40] J.A. Gadsden, The Infrared Spectra of Minerals and Related Inorganic Compounds, in:
, Butterworth, London, 1975.
[41] S.J. Gregg, K.S.W. Sing, Adsorption, Surface Area and porosity, 2nd ed., Academic Press, New York, 1982.

[42] A. Shimojima, K. Kuroda, Direct formation of mesostructured silica-based hybrids from novel siloxane oligomers with long alkyl chains, Angewandte Chemie-International Edition, 42 (2003) 4057-4060.
[43] V.A. Gerasin, F.N. Bakhov, N.D. Merekalova, Y.M. Korolev, H.R. Fischer, E.M. Antipov, Structure of surfactant layers formed on Na^+ montmorillonite and compatibility of the modified clay with polyolefins, Polymer Science Series A, 47 (2005) 954-967.
[44] C.H. Giles, T.H. MacEwan, S.N. Nakhwa, Studies in adsorption. Part XI. A system of classification of solution adsorption isotherms, and its use in diagnosis of adsorption mechanisms and in measurement of specific surface areas of solids, J. Chem. Soc., (1960) 3973-3993.
[45] J.S. Mattson, H.B. Mark, Jr., Activated Carbon-Surface Chemistry and Adsorption from Solution, in, Marcel Dekker, Inc., New York, 1971.
[46] R. Rajeswari, S. Kanmani, A study on degradation of pesticide wastewater by TIO_2 photocatalysis, Journal of Scientific & Industrial Research, 68 (2009) 1063-1067.

List of Figures

Fig 1. XRD patterns of samples: AF– pure γ-Al_2O_3 fibres; AF(A) – acid washed fibres; AFC8(50) and AFC8(100) – OTES grafted samples; AFC1(50) and AFC1(100) CPTES grafted samples.

Fig 2. FTIR spectra of samples: AF(A) – acid washed fibres; AFC8(50) and AFC8(100) – OTES grafted samples; AFC1(50) and AFC1(100) CPTES grafted samples.

Fig 3. a) Transmission electron micrograph of AF(A); b) and c) micrographs of AFC8(100) and AFCI(100) respectively.

Fig 4. Samples (a) (b) and (c) are TGA and DTG curves of AF(A), AFC1(100) and AFC8(100) respectively.

Fig 5. N_2 adsorption/desorption isotherms for grafted and non- grafted γ-Al_2O_3 fibres: AF(A) – acid washed fibres; AFC8(50) and AFC8(100) – OTES grafted samples; AFC1(50) and AFC1(100) – CPTES grafted samples.

Fig 6. The profile of water droplets on the surface of the pellets form of modified γ-Al_2O_3 fibres: (a) AF(A) – acid washed; (b) AFC1(100) – CPTES grafted samples; (c) AFC8(100) – OTES grafted samples respectively.

Fig 7. Solid-state ^{29}Si MAS NMR spectra: a) AFC8 – CPTES grafted samples; (b) AFC1 – OTES grafted samples**.**

Fig 8. The schematical diagrams of γ-Al_2O_3 fibres before (a) and after grafting (b).

Fig 9. Adsorption isotherms of alachlor(a) and Imazaquin(b).

Fig 10. The amount of uptake was plotted against the square root of time.

Fig 11. A schematical view of grafted surface and possible interaction with pollutants.

447

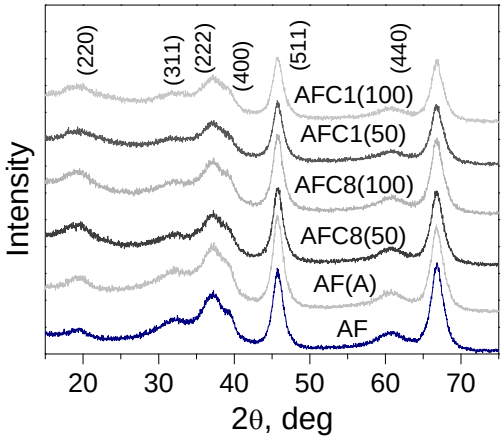

448
449 **Fig 1.**

450

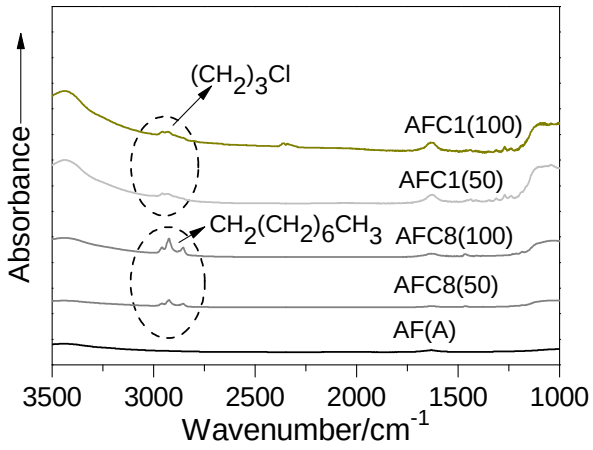
(CH2)3Cl
AFC1(100)
AFC1(50)
CH2(CH2)6CH3
AFC8(100)
AFC8(50)
AF(A)
Absorbance
3500
3000
2500
2000
1500
1000
Wavenumber/cm-1

Fig 2.

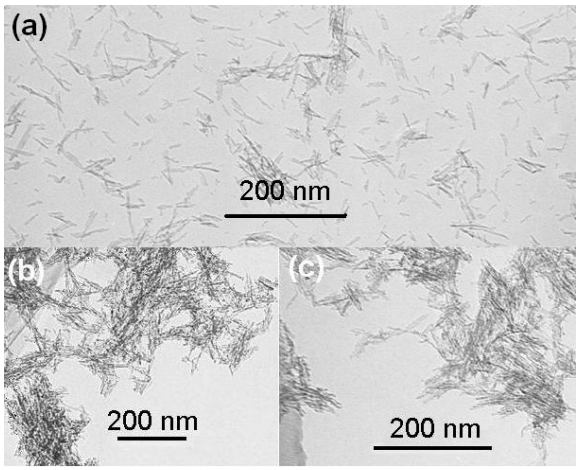

Fig 3.

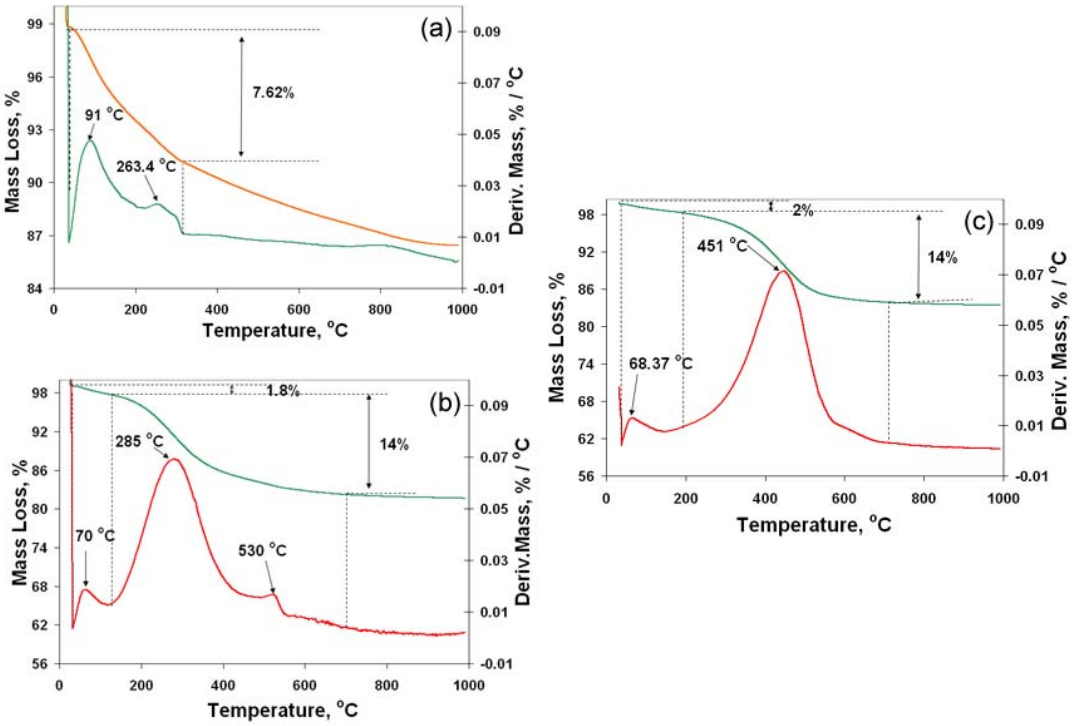
(a)
7.62%
91 °C
263.4 °C
Mass Loss, %
Deriv. Mass, % / °C
Temperature, °C
(b)
1.8%
14%
285 °C
70 °C
530 °C
Mass Loss, %
Deriv.Mass, % / °C
Temperature, °C
(c)
2%
14%
451 °C
68.37 °C
Mass Loss, %
Deriv. Mass, % / °C
Temperature, °C

Fig 4.

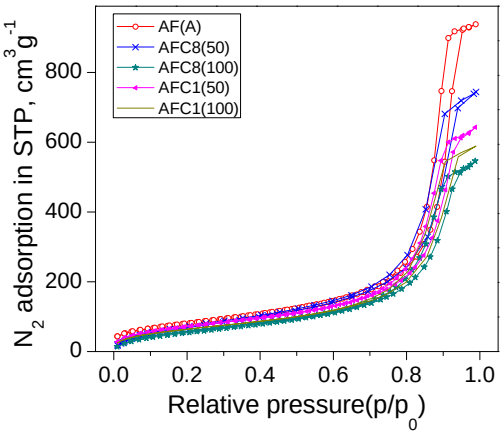
AF(A)
AFC8(50)
AFC8(100)
AFC1(50)
AFC1(100)
N2 adsorption in STP, cm3 g-1
0
200
400
600
800
0.0
0.2
0.4
0.6
0.8
1.0
Relative pressure(p/p0)

Fig 5.

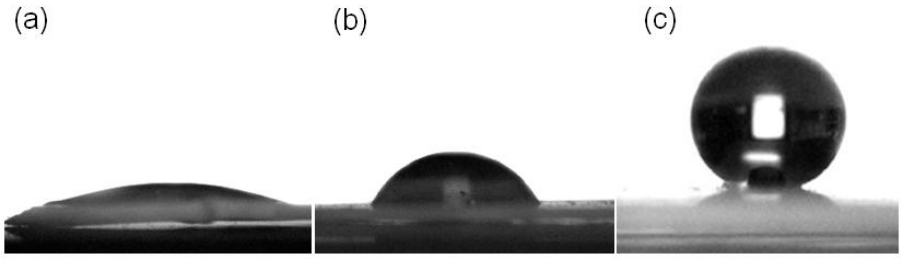

Fig 6.

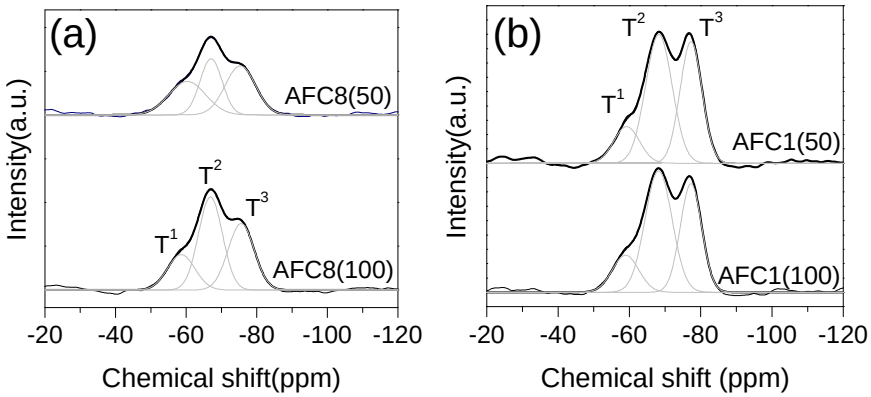
(a)
AFC8(50)
T2
T3
T1
AFC8(100)
Intensity(a.u.)
-20 -40 -60 -80 -100 -120
Chemical shift(ppm)
(b)
T2
T3
T1
AFC1(50)
AFC1(100)
Intensity(a.u.)
-20 -40 -60 -80 -100 -120
Chemical shift (ppm)

Fig 7.

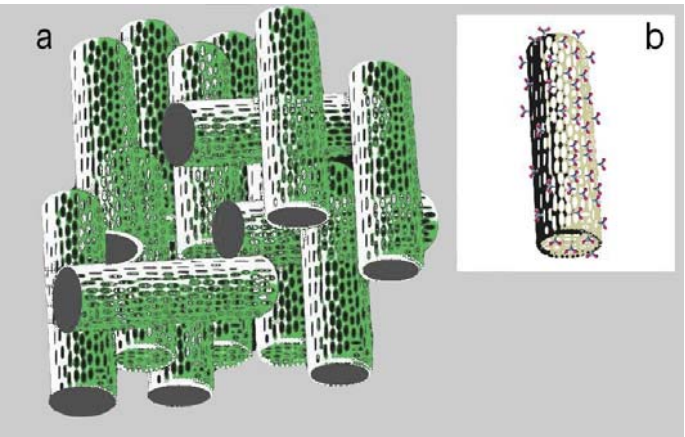

Fig 8.

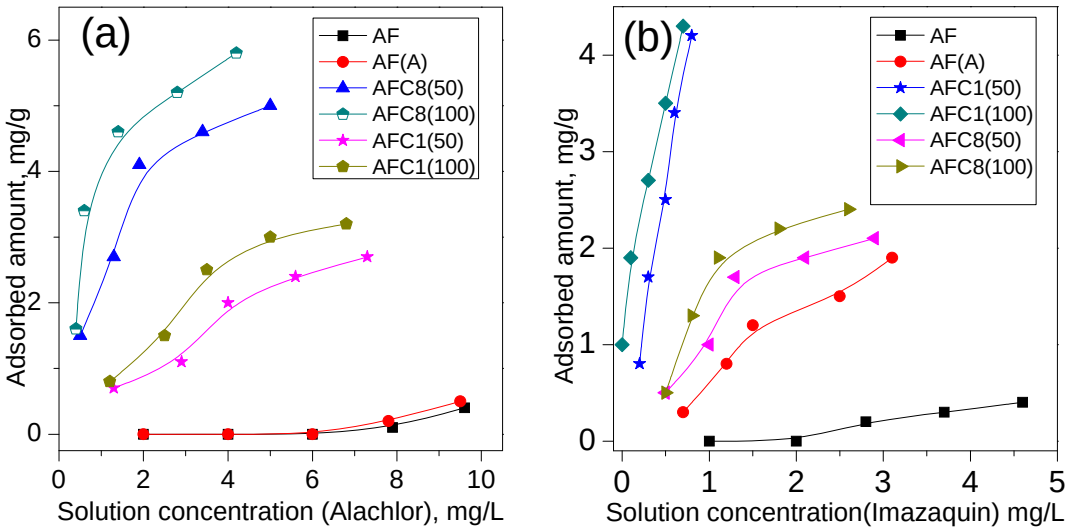
(a)
AF
AF(A)
AFC8(50)
AFC8(100)
AFC1(50)
AFC1(100)
Adsorbed amount, mg/g
Solution concentration (Alachlor), mg/L
(b)
AF
AF(A)
AFC1(50)
AFC1(100)
AFC8(50)
AFC8(100)
Adsorbed amount, mg/g
Solution concentration(Imazaquin) mg/L

Fig 9.

496

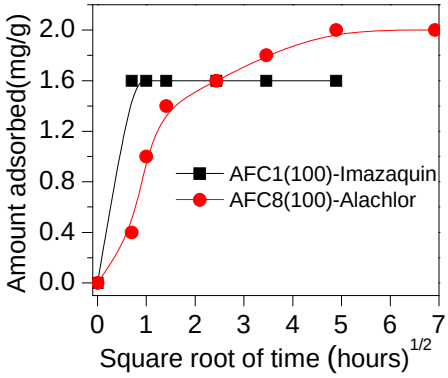

497

498 **Fig 10.**
499

500

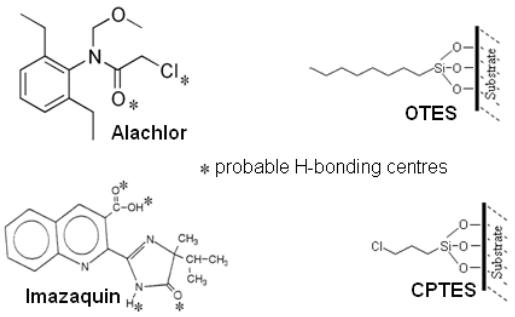

501

502 **Fig 11.**

503

504

505

List of Tables

Table1. Specific surface area, pore volume and mean pore diameter of samples: AF and AF (A) as synthesized and acid washed γ-Al_2O_3 respectively; AFC8 (50) and AFC8 (100) – CPTES grafted samples; AFC1 (50) and AFC1 (100) – OTES grafted samples.

Table 2.

			mean D [46]	
Samples	$S_{BET}(m^2.g^{-1})$	V_p[a]$(cm^3.g^{-1})$	BET[b]	BJH[c]
AF(F)	292	1.45	19.9	14.0
AFC1(50)	266	1	14.9	12.5
AFC1(100)	232	1	15.7	11
AFC8(50)	252	1	16.5	11.4
AFC8(100)	217	0.84	15.3	10.7

[a] Single point adsorption total pore volume of pores at P/P_0 0.99. [b] Adsorption average pore diameter(4V/A by BET). [C] Barrett–Joyner–Halenda(BJH) desorption average pore diameter(4V/A).